

A Preliminary Study on Impact of Landslide Debris on Flexible Barriers

GEO Report No. 309

H.W. Sun & R.P.H. Law

**Geotechnical Engineering Office
Civil Engineering and Development Department
The Government of the Hong Kong
Special Administrative Region**

A Preliminary Study on Impact of Landslide Debris on Flexible Barriers

GEO Report No. 309

H.W. Sun & R.P.H. Law

**This report was originally produced in April 2012
as GEO Technical Note No. TN 1/2012**

© The Government of the Hong Kong Special Administrative Region

First published, May 2015

Prepared by:

Geotechnical Engineering Office,
Civil Engineering and Development Department,
Civil Engineering and Development Building,
101 Princess Margaret Road,
Homantin, Kowloon,
Hong Kong.

Preface

In keeping with our policy of releasing information which may be of general interest to the geotechnical profession and the public, we make available selected internal reports in a series of publications termed the GEO Report series. The GEO Reports can be downloaded from the website of the Civil Engineering and Development Department (<http://www.cedd.gov.hk>) on the Internet. Printed copies are also available for some GEO Reports. For printed copies, a charge is made to cover the cost of printing.

The Geotechnical Engineering Office also produces documents specifically for publication in print. These include guidance documents and results of comprehensive reviews. They can also be downloaded from the above website.

These publications and the printed GEO Reports may be obtained from the Government's Information Services Department. Information on how to purchase these documents is given on the second last page of this report.



H.N. Wong
Head, Geotechnical Engineering Office
May 2015

Foreword

This Technical Note presents a preliminary study of possible mechanisms involved in impact of debris flows on flexible landslide debris-resisting barriers and the dynamic interaction process.

This Note covers a review of design approaches put forward in the literature and adopted by the construction industry for debris-resisting flexible barriers. Based on insights from results of physical experiments and advanced numerical models, two possible debris deposition mechanisms involved in the impact of landslide debris on flexible barriers are identified. The observations may help designers to gain a better appreciation of the possible dynamic interaction between a debris-resisting flexible barrier and the landslide debris, and provide a basis for further development work in this subject area.

The study was carried out by Dr H.W. Sun and Mr R.P.H. Law. Mr H.N. Wong, Mr K.K.S. Ho, as well as Mr Anthony Lam and colleagues in the Standards and Testing Division provided comments and suggestions on the preliminary draft of this Note. Professor Oldrich Hungr of the University of British Columbia, Canada also reviewed the draft of this Note. All support and contributions are gratefully acknowledged.



Y.K. Shiu

Chief Geotechnical Engineer/Standards and Testing

Abstract

This Technical Note presents findings from a preliminary study on the interaction mechanisms involved in the impact of landslide debris of different characteristics on flexible landside-resisting barriers. Based on observations in field and laboratory tests and with the support of numerical modelling using the distinct element code PFC^{3D}, two possible debris deposition mechanisms involved in the impact of landslide debris on flexible barriers are identified. An initial quantitative assessment of the possible level of kinetic energy of the portion of landslide debris transferred to the barrier upon impact has been undertaken for the two deposition mechanisms, which may be taken forward further with suitable refinements with a view to formulating a design framework. Further work to examine the debris impact and interaction mechanisms and to reduce uncertainty in design assessments of barriers is recommended. The preliminary assessment presented may also help designers to gain a better appreciation of possible dynamic interaction between a flexible barrier and landslide debris upon impact.

Contents

	Page No.
Title Page	1
Preface	3
Foreword	4
Abstract	5
Contents	6
List of Tables	8
List of Figures	9
1 Introduction	10
2 Existing Approaches	10
2.1 Conventional Lumped Mass Model	10
2.2 Wartmann & Salzmann (2002) Method	11
2.3 Wendeler et al (2010) Method	11
3 Preliminary Appraisal	12
4 Numerical Modelling of Debris Impact and Deposition	13
4.1 Model Setup and Analysis	13
4.2 Discussions of Results	15
5 Landslide Debris Deposition Mechanisms	18
6 Impact Energy	19
6.1 Pile-up Mechanism	19
6.2 Run-up Mechanism	24
7 Debris-barrier Interaction	27
7.1 Characterisation of Barrier Responses	28
7.2 Balance of Forces and Barrier Deflection	28
8 Discussions	29

	Page No.
9 Conclusions	31
10 References	32
Appendix A: Worked Examples	34
Appendix B: Comparison between Analytical Solutions and Finite Difference Calculations for Debris-barrier Interaction Mechanisms	41

List of Tables

Table No.		Page No.
4.1	Parameters Adopted in Numerical Simulations Using PFC ^{3D}	15
6.1	Analytical Solutions for Impact of Landslide Debris on Flexible Barriers	27

List of Figures

Figure No.		Page No.
4.1	Setup of Numerical Model	14
4.2	Deposition of Landslide Debris behind a Flexible Barrier Indicating (a) A Pile-up Mechanism Involving ‘Viscous’ Material, and (b) A Run-up Mechanism Involving ‘Frictional’ Material	16
5.1	Schematic Diagrams of Landslide Deposition Mechanisms of Landslide Debris Impacting on Flexible Barrier	18

1 Introduction

Flexible steel mesh fences as landslide debris-resisting barriers are often preferred options for mitigation of natural terrain landslides in Hong Kong, as flexible landslide barriers are more adaptive and buildable on steep hillside than rigid barriers. Flexible barriers have been reported in the literature as being capable of retaining debris up to about 750 m³ in volume over several impacts (e.g. Roth et al, 2004). However, the typical volume of landslide debris involved in most of the events was in the range of 100 m³ to 200 m³ as far as direct frontal impact loading on the tensioned steel mesh fence is concerned. Flume tests of landslide debris impacting on proprietary steel mesh fences (Duffy, 2008) indicate that this type of barrier can retain up to about 10 m³ of debris travelling at velocities of up to about 9 m/s. Experience of application of such tensioned steel mesh fences to resist the impact of sizeable landslides is limited and the performance of prototype tensioned steel mesh fences has not been fully verified in the field. An overview on the use of flexible barriers in mitigating natural terrain landslides has been summarised by Shum et al (2011). Some of the design approaches proposed recently in the literature (e.g. Wartmann & Salzmann, 2002) appear to involve projection of data obtained from relatively small-scale tests on the key design assumptions (e.g. the duration of impact by debris of a given discharge rate), which can be open to questions. Recently, further field test data have become available and a new approach for assessing structural adequacy of the main ropes was developed (Wendeler et al, 2010).

Although it is useful to obtain data and observations from field tests on the performance of flexible barriers under impact of landslide debris, it would be necessary to examine closely the mechanisms of landslide deposition behind the flexible barrier as well as possible interaction between the landslide barrier and the impacting landslide debris under different landslide conditions for well defined boundary conditions. This Technical Note presents a review of the existing approaches available in the literature and adopted by the construction industry for assessment of flexible barriers under impact of landslide debris. A simplified assessment of two possible debris deposition mechanisms involved in the impact of landslide debris on flexible barriers was developed through an examination of the results of numerical models on the different mobility characteristics of landslide debris. The assessment provides a potential preliminary approach in quantifying the possible range of impact energy to be absorbed by flexible barriers when they are impacted by landslide debris of different characteristics. Some worked examples of this new approach are presented to illustrate its possible applications.

2 Existing Approaches

2.1 Conventional Lumped Mass Model

In this model, the entire landslide mass is assumed to interact with the barrier. The total kinetic energy to be absorbed by the barrier (E_B) is given below:

$$E_B = \frac{mU^2}{2} = \frac{\rho V U^2}{2} \dots\dots\dots (2.1)$$

where m = total active mass of landslide debris
 U = velocity of landslide debris

- V = total active volume of landslide debris
- ρ = mass density of landslide debris

However, this is likely to be too conservative for a sizeable long-runout landslide and it is not feasible to provide a flexible barrier to absorb all the kinetic energy of the entire active landslide mass. We can expect that a notable portion of the total kinetic energy of the landslide mass would be dissipated through inelastic deformation of the debris on impact with the barrier as well as on the debris trapped behind the barrier. Once the frontal portion of the landslide is arrested by the barrier, the bulk of the landslide debris trapped behind the barrier would interact with the subsequent portion of the incoming landslide debris and eventually the barrier will not be involved in taking up further debris impact loads.

2.2 Wartmann & Salzmann (2002) Method

Wartmann & Salzmann (2002) reported an approach largely developed from flume tests in USGS (maximum active debris volume about 10 m^3), where the duration of interaction between landslide debris and flexible barrier was measured. Based on this, the energy rating for the flexible barrier (E_B) can be expressed as follows:

$$E_B = \frac{m_a U^2}{2} = \frac{\rho Q T_s U^2}{2} \dots\dots\dots (2.2)$$

- where m_a = active mass of landslide debris involved during the interaction with the deflection of the barrier and $m_a = \rho Q T_s$
- Q = discharge rate (in m^3/sec)
- T_s = duration of ‘effective’ interaction/impact (in seconds)

This can be viewed as follows: the active mass is taken as the volume of the landslide debris that may pass through the initial position of the barrier over the duration of ‘effective’ interaction/impact as if there were no barrier.

Based on the test results, Wartmann & Salzmann (2002) recommended that the maximum duration of impact affecting the barrier (T_s) should be taken as 4 seconds.

The Wartmann & Salzmann (2002) method appears to have been developed based on conservation of energy (viz. impact energy absorbed by the deforming barrier = kinetic energy of active mass of landslide debris over the duration of interaction ($0.5 m_a U^2$)). However, no further analysis or discussion of the basis of their recommendations was made by Wartmann & Salzmann (op cit).

2.3 Wendeler et al (2010) Method

Wendeler et al (2010) back analysed the rope force distribution collected from recent field tests conducted by one of the steel mesh fence manufacturers and suggested various distributions of earth pressure exerted on flexible barriers due to deposition of landslide debris behind the barrier for structural design of the barrier. Sizing of the main ropes and other structural elements can be obtained through detailed structural analyses of the barrier system

as a cable structure. Using this approach, expert structural engineering input is required for the structural design of the barrier system. With this approach, the sizing/structural design of the flexible barrier is different from other steel mesh fences currently marketed by other manufacturers, which have traditionally been designed, constructed and verified according to the level of impact energy by a boulder or rock fall.

3 Preliminary Appraisal

Flexible barrier is an engineering structure designed to retain approaching landslide debris as a landslide mitigation measure. The barrier is to be designed to maintain its overall stability and structural integrity when it is subjected to the effects of impact and deposition of debris behind it. The structural adequacy/capacity of the barrier can be assessed in terms of its ability to take up the impact loading and applied forces upon the impact of the landslide debris onto the barrier.

For the design of landslide debris-resisting rigid barriers, existing guidelines and recommendations are available (Lo, 2000). In general, the barrier is to be designed to withstand quasi-static impact pressure assessed from the consideration of intensity and velocity of the influx of the landslide debris as well as other external loads (e.g. static earth pressure from the debris deposited behind the wall). Forces due to impact of boulder inclusions are usually assessed based on the assumption of elastic impact and reduced by a large empirical modification factor.

For the design of flexible barrier against impact of landslide debris, the approach proposed by Wendeler et al (2010) appears to be similar to the design methodology for rigid barriers. Structural capacity of the barrier is to be assessed for combinations of quasi-static impact pressure from impact of the approaching landslide debris as well as from the 'static' earth pressure from the debris deposited behind the barrier. The challenge of this approach is probably the structural assessments needed to verify the performance of the flexible and highly deformable structure and the adequacy of all its structural components. Based on equilibrium of forces, the existing semi-empirical approach for assessment of impact of boulder on rigid barrier cannot be readily applied for impact of boulder on a flexible barrier.

For design of boulder fence, it is traditional to size the barrier by reference to its capability in taking up the impact of the boulder according to its kinetic energy prior to impact. The interaction and the mechanism involved in boulder impact on a flexible barrier is very complex, which may involve large localised deformation of the steel wire mesh, mobilisation of brake rings/elements as well as the cables. The performance of flexible rockfall barrier is usually verified using full-scale field tests, although numerical models can also be used in research and development work (Grassl et al, 2002).

Using an energy approach, the sizing of flexible barriers in terms of impact energy is not straightforward. As discussed in Sections 2.1 and 2.2, the kinetic energy of the landslide mass involved in impact of the barrier could be estimated based on the definition of the 'active' mass, which is taken as the volume of the landslide debris that may pass through the initial position of the barrier over the duration of interaction/impact as if there were no barrier. Although this may not be unreasonable from an engineering application point of view, the performance of the barrier in terms of force distribution and mobilisation of the load-carrying

capacity of the barrier during the impact of the landslide debris requires further studies. A flexible barrier that is verified to a certain level of energy capacity for boulder impact may not be able to justify the same level of energy capacity for impact of landslide debris as the behaviour of the barrier will not be the same. On the other hand, the energy approach, discussed in Sections 2.1 and 2.2 involves a conservative assumption that the impact energy on the barrier is equal to the kinetic energy of the ‘active’ landslide mass, viz. loss of kinetic energy through inelastic impact (and deformation) of the landslide debris is ignored. This may well over-estimate the actual impact energy involved in the event.

Overall, the above points to the need for a better appreciation and understanding of the deposition mechanism of landslide debris behind a flexible barrier as well as their interactions.

4 Numerical Modelling of Debris Impact and Deposition

Particle Flow Code in Three Dimensions (PFC^{3D}) (Itasca, 2005) is a numerical simulation tool that models the motion and interaction of spherical particles by means of the Distinct Element Method (DEM) (Cundall & Strack, 1979). In this Technical Note, the results of a preliminary study on the deposition behaviour of debris flow impacting a flexible barrier are presented. Two possible limiting debris mobility regimes of debris flows/landslides debris upon impact with a compressible (flexible) barrier are studied by numerical simulations. The local rheology giving rise to two possible limiting debris movement regimes are simulated in the Discrete Elements Model by means of the contact behaviour between interacting discrete elements (see Section 4.1). Although these two limiting flow regimes may not cover the whole spectrum of debris flow conditions (e.g. debris flood that may go beyond these two regimes modelled using the Discrete Element Method), they serve to identify the associated limiting debris deposition conditions and provide insights on possible design approaches for debris impact on flexible barriers.

It should be pointed out that the purpose of the numerical simulations is to diagnose the debris deposition process and the possible dynamic effect on the flexible barrier in a qualitative manner, given the complexity of the dynamic behaviour of debris flow, the uncertainty in model parameters and limitations of the numerical code in replacing the complex rheological properties of the materials involved.

4.1 Model Setup and Analysis

Figure 4.1 shows the setup of the numerical model. The two side walls and the channel floor are modelled using rigid wall elements and the landslide debris is represented by a cluster of spherical elements. Two conditions of landslide debris movement characteristics are modelled in this assessment by adopting different model parameters which simulate, in a qualitative manner, landslide debris travelling at various velocities upon its impact with a compressible (flexible) barrier. A relatively fast moving debris is modelled with a ‘viscous material’ by assigning a viscous normal and shear damping of 0.4 and a nominal inter-particle friction angle of 0.1° that provide viscous contact/interaction behaviour between discrete elements. A relatively slow moving debris is modelled with a ‘frictional material’ by assigning an inter-particle friction angle of 14° and a nominal viscous normal and

shear damping of 0.2 that provide a frictional contact/interaction behaviour between discrete elements. For simplicity, interface friction between the particles and the sliding surface is taken to be identical to the inter-particle friction angle. However, with the numerical code PFC^{3D}, viscous damping that is allowed for between particles could not be applied to the interface between the particles and the sliding surface. In this respect, viscous behaviour at the boundary of channel fluid flow, especially for turbulent flow, has not been modelled in the present study.

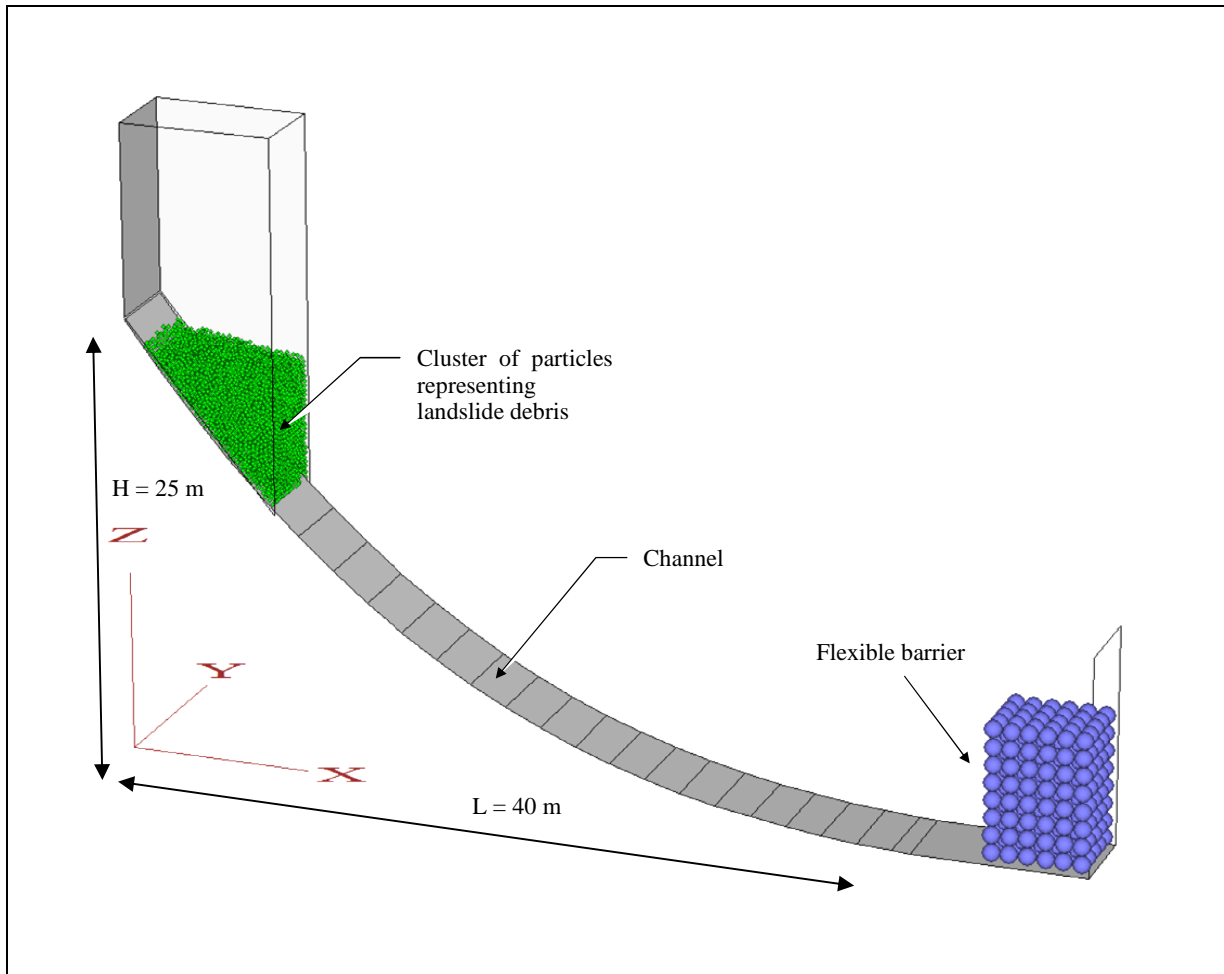


Figure 4.1 Setup of Numerical Model

Two matrices of spherical elastic particles were used to simulate the flexible barrier, namely the spring matrix and filler matrix. The spring matrix consists of elastic particles in a cubic packing designed to pick up the impact load by the debris during the impact process. The filler matrix is made up of smaller particles to fill up the voids within the spring matrix to prevent particles within the flow mass to penetrate excessively into the spring matrix.

Table 4.1 summarises the parameters used for the numerical analysis. The approach and details of the numerical models presented are similar to that used by Law et al (2007) in back analyses of physical flume tests.

Table 4.1 Parameters Adopted in Numerical Simulations Using PFC^{3D}

Parameter	Value
Number of balls	Landslide debris: 8,000 Flexible barrier: 380
Ball radius	Landslide debris: 0.135 m Flexible barrier: 0.5 / 0.33 m
Density	Landslide debris: 1,800 kg/m ³ Flexible barrier: 100 kg/m ³
Mass of material representing landslide debris	150,000 kg
Normal and tangential ball stiffness	Landslide debris: 10 ⁶ N/m Flexible barrier: 10 ⁶ N/m
Internal and interface friction angle	Viscous material: 0.1° Frictional material: 14°
Local damping	Landslide debris: 0.05 Flexible barrier: 0.7
Viscous normal and shear damping	Viscous material: 0.4 Frictional material: 0.2 Flexible barrier: 0
Stiffness of model boundaries (walls)	Normal: 10 ⁸ N/m Tangential: 10 ⁸ N/m

4.2 Discussions of Results

Figure 4.2 shows the deposition process of landslide debris with different movement characteristics comprising spherical particles with two different types of interaction models (i.e. ‘viscous’ and ‘frictional’) impacting on the flexible barrier. The arrows shown on each of the particles indicate the movement direction and its velocity. As revealed by the results of PFC^{3D} models, two possible deposition mechanisms are involved upon the impact of landslide debris on a flexible barrier depending on the different movement characteristics as a result of the assumptions adopted for the interaction between particles or the characteristics of the debris represented by the models.

For the model adopting ‘viscous’ behaviour between particles, landslide debris appears to be relatively fast moving (moving at an average velocity of about 6 m/s along the 40 m length of approach channel before the first impact) and piled up against the barrier wall following impact. In this case, the flowing sheet of debris makes a 90-degree turn and shoots up against the barrier wall until the kinetic energy of the debris is fully consumed by the gain in potential energy. Subsequent influx of debris appears to continue to pile up against this stationary block of debris behind the barrier wall. This interaction mechanism is termed ‘pile-up’ mechanism in this Note.

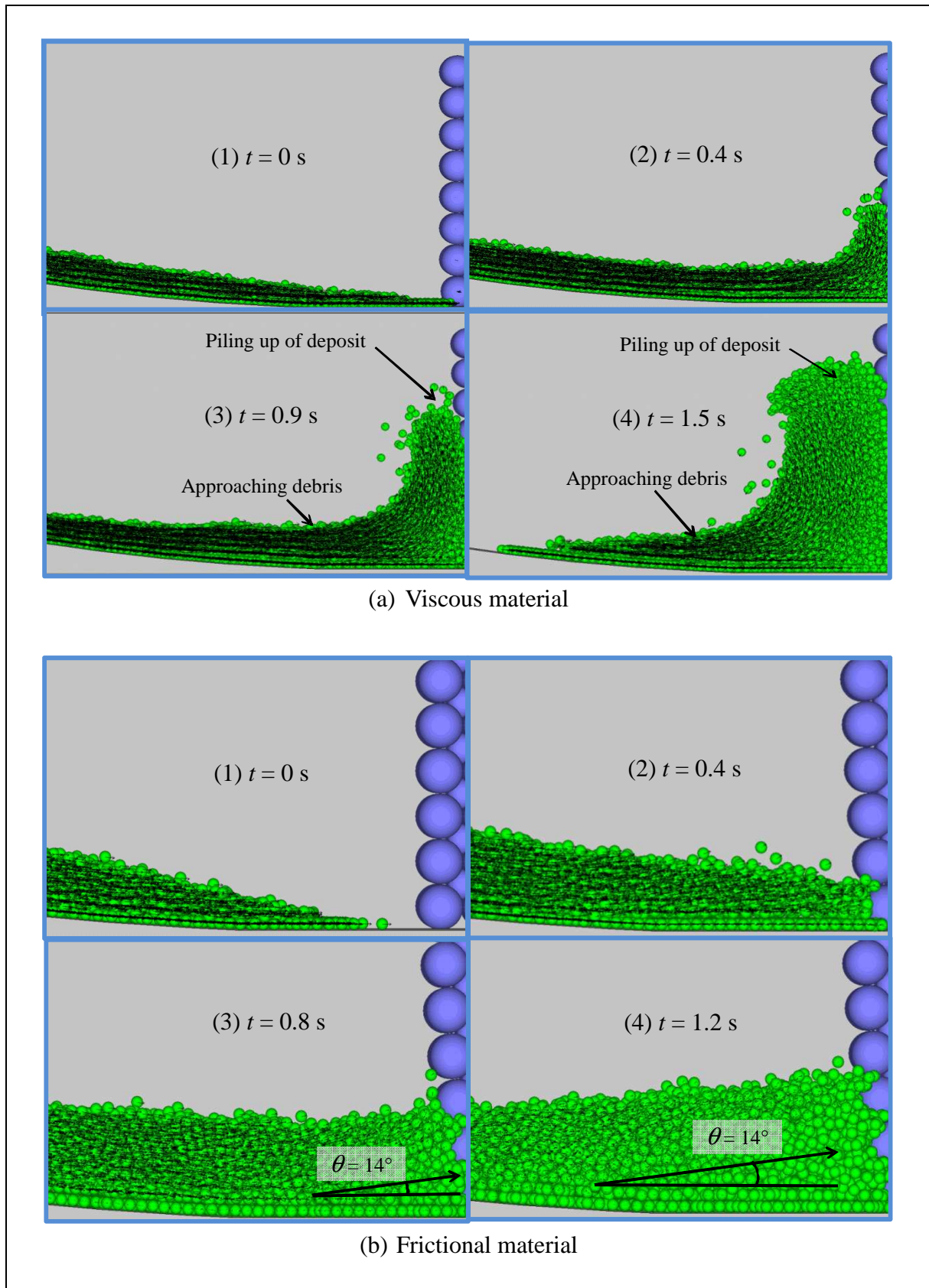


Figure 4.2 Deposition of Landslide Debris behind a Flexible Barrier Indicating (a) A Pile-up Mechanism Involving ‘Viscous’ Material, and (b) A Run-up Mechanism Involving ‘Frictional’ Material

For the model adopting ‘frictional’ behaviour between particles, the landslide debris appears to move at a lower velocity (moving at an average velocity of about 5 m/s along the approach channel before the first impact) and a different deposition mechanism prevails. In this case, a debris mass appears to have deposited behind the barrier wall following impact and form a wedge of stationary mass. This wedge of relatively stationary material forms a sloping ramp with a gradient that approximately equals to the internal friction angle (or the angle of repose) of the debris. Subsequent influx of debris material runs up this ramp before it impacts on the barrier wall and becomes part of the enlarging wedge of stationary mass. As a result, the kinetic energy of the later portion of the debris influx would be reduced substantially whilst it overcomes the increased elevation over the portion of the wedge of stationary mass before it reaches the barrier wall. This interaction mechanism is termed ‘run-up’ mechanism in this Note.

It should be noted that the PFC model used is not designed to simulate the performance of the flexible barrier on impact with the landslide debris and did not represent the mechanisms of energy absorption by the barrier. It should also be noted that the results of the numerical model PFC^{3D} used in this analysis may not be completely realistic in modelling the complex energy dissipation mechanisms involved in an impact of landslide debris on a flexible barrier (e.g. energy dissipation through inelastic internal deformation/distortion of the compressible/deformable landslide debris, interaction and transfer of forces between the landslide debris and the barrier following initial impact) to quantify the impact energy on the barrier. Apart from the consideration of the change in kinetic and potential energy discussed above, some energy may also be consumed through particle interaction (e.g. collision and sliding), especially for the pile-up mechanism as the motion is fairly turbulent. It can also be observed that the particles during the entire runout process are fairly dispersed (due to the number of particles used to limit the computing resources required), with some rolling and bouncing. This may render the model less representative particularly in simulating wet debris flows. In this respect, other 3-D continuum models, e.g. smooth particle hydrodynamic model or finite volume model, could be more realistic.

The above interaction mechanisms are relative to the flexible barrier involving the portion of landslide debris impacting and depositing behind the flexible barrier, which in a global sense deforms/deflects forward due to the forces exerted by the landslide debris as the forward moving velocity of the landslide debris is, in general, much greater than the rate of forward movement of the barrier.

Additional analyses have also been carried out to examine the sensitivity of the parameters and approach adopted. It is noted that the characteristics of the impacting debris are not unduly sensitive to the rheological parameters of the particles as well as the ‘stiffness’ of the model flexible barrier adopted, provided the barrier is relatively flexible as compared with the stiffness of the landslide debris. In fact, impact of landslide debris on a rigid barrier could well be more complicated than that on a flexible barrier, as the dynamic interaction and impact pressure is affected by the propagation of shock waves, similar to observations made of impact on snow avalanche protection dam (Jóhannesson et al, 2009) and modelling of debris run-up against protection dams and barriers (Mancarella & Hungr, 2010).

5 Landslide Debris Deposition Mechanisms

The two landslide debris deposition mechanisms identified through the PFC^{3D} numerical models, viz. (a) pile-up and (b) run-up, are consistent with observations from physical/field tests, including the USGS flume tests on wet slurry/debris flows materials as well as dry granular flows in laboratory flume tests (Law, 2008).

In the pile-up mechanism, the frontal portion of the landslide debris shoots up against the barrier wall stem upon impact, and subsequently the relatively stationary debris piled up behind the barrier wall is impacted by the latter portion of the landslide debris. The latter portion of the landslide debris continues to exert pressure on the portion of debris piled up behind the barrier (Figure 5.1a).

In the run-up mechanism, landslide debris would slide along the top surface of a wedge of ‘relatively stationary’ debris (i.e. the frontal portion of the landslide debris mass successfully arrested by the barrier) and continue to impact directly on the barrier (Figure 5.1b). The impact on the barrier will cease when the subsequent flow of landslide debris stops along its run-up path towards the barrier.

It should be noted that the two possible scenarios of landslide debris movement characteristics and deposition mechanisms as observed in this study were obtained with the use of different model parameters, qualitatively simulating landslide debris travelling at different velocity on its impact with the barrier. With continued discharge of debris with varied movement characteristics, it is possible that the deposition mechanism may change over the duration of impact or different pulses of impact (e.g. change from a pile-up mechanism to a run-up mechanism).

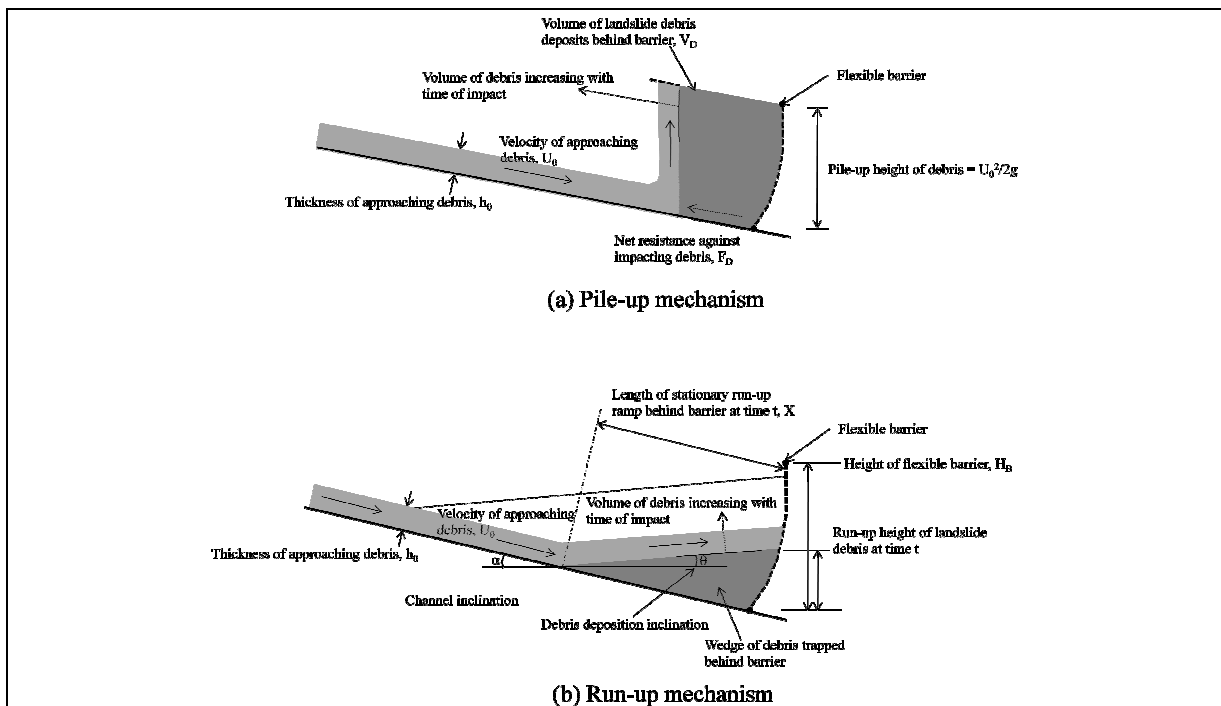


Figure 5.1 Schematic Diagrams of Landslide Deposition Mechanisms of Landslide Debris Impacting on Flexible Barrier

6 Impact Energy

For both scenarios, the volume of moving landslide debris involved directly in the interaction with the flexible barrier is limited and there is a duration when the frontal portion of the landslide debris interacts with the barrier. A notable proportion of the total kinetic energy of the landslide debris will be lost through inelastic deformation of the debris on impact with the barrier and with the debris trapped behind the barrier. In principle, impact energy rating required for the flexible barrier may be related to the kinetic energy of the ‘frontal portion’ for the landslide debris involved over the duration of impact/interaction with the flexible barrier. However, it is difficult to define precisely both the spatial and temporal demarcations of this frontal portion of the landslide debris. Furthermore, the mechanism involved in absorption of impact energy for impact of boulder on a flexible steel fence (Grassl et al, 2002) will be different from that involved in impact of landslide debris on a flexible barrier. An initial assessment of the kinetic energy of the landslide debris that could interact with the barrier is presented in the following sections.

6.1 Pile-up Mechanism

To simplify the illustration of this deposition mechanism, the discharge rate (Q_0) and velocity (U_0) of the approaching landslide debris mass are assumed to be constant. The analysis adopts the Lagrangian approach and the frame of reference is the location of the flexible barrier, which moves forward under the impact pressure of the landslide debris.

Assuming that the barrier is able to maintain overall stability, the forces exerted on the landslide debris behind the barrier by the impacting debris would be balanced by the net restoring forces provided by the basal sliding resistance of debris deposited behind the barrier and the reaction/resistance provided by the flexible barrier. An equilibrium equation considering the rate of change of momentum of the approaching debris can be established as follows:

$$\frac{dM}{dt} = F_D + F_B \dots\dots\dots (6.1)$$

- where M = momentum of approaching landslide debris at time t
- F_D = net resistance acting on the landslide debris deposit behind the barrier
- F_B = reaction force provided by the barrier

The net resistance provided by the landslide debris deposited behind the barrier is the basal resistance subtracted by the body force vector of the landslide debris in the direction of the debris channel behind the barrier. The net resistance acting on the landslide debris deposited behind the barrier may be taken as follows:

$$F_D = (\mu \cos \theta - \sin \theta) \rho g V_D \dots\dots\dots (6.2)$$

- where μ = $\tan \phi$ (ϕ is the interface friction between the landslide debris and the channel base)
- ρ = bulk density of the landslide debris deposit
- g = gravitational acceleration

- θ = horizontal angle of the channel base behind the barrier
 V_D = volume of landslide debris deposited behind the barrier

In case the debris runout channel is very steep and by ignoring the contribution of the barrier in holding the static equilibrium of the debris deposited behind it, the basal resistance on the landslide debris deposited behind the barrier may not be available for the ‘protection’ of the barrier.

The lateral compaction force on the stationary landslide debris trapped behind the barrier due to the impact of the debris arriving at a velocity (U_0) from upstream is as follows:

$$F_A = \gamma \rho h_0 w U_0^2 \dots\dots\dots (6.3a)$$

- where h_0 = thickness of the approaching debris (assuming a direct hit on the barrier is made at 90°)
 w = width of the landslide debris (assuming a rectangular cross-section)
 γ = dynamic pressure coefficient considering differences between the change in momentum when a Newtonian fluid impacts on a rigid wall as compared with that from a landslide debris

The dynamic impact pressure of landslide debris on a barrier is another frontier of our current knowledge. In the literature, the dynamic pressure coefficient (γ) is reported to vary between 0.5 and 3 to 6, depending on different practices and considerations. Largely based on reports of field measurements in China and a review of laboratory experiments of impact of debris flows on rigid structures, Lo (2000) recommended that a minimum factor of 3 should be adopted for debris impacting on rigid barriers, partly due to presence of hard lumps in the debris mass. It is arguable if this dynamic pressure coefficient of 3 is applicable for impact of landslide debris on a deforming flexible barrier or on deformable landslide debris deposited behind the barrier upon impact of the landslide debris.

From hydrodynamic considerations, a dynamic pressure coefficient of 2 is applicable for Equation 6.3a if the influx makes a 180° turn upon impact with an object and the dynamic pressure coefficient of unity is applicable if the incoming debris is deflected by 90° . It is, in fact, similar to the model of debris deposition observed.

More recently, Hübl et al (2009) reviewed a wide range of experimental and field measurements, including their own field measurements and tests as well as those covered by Lo (2000) and suggested an alternative approach. This approach relates impact pressure to the hydrodynamic characteristics of the debris flow by correlating impact pressure with the Froude number, F_d ($F_d = U / (g h)^{0.5}$), of the flow of landslide debris. Adopting the approach suggested by Hübl et al (op cit), Equation 6.3a can be modified as follows:

$$F_A = (5 g^{0.6} h_0^{0.6} U_0^{-1.2}) \rho h_0 w U_0^2 = 5 \rho g^{0.6} w h_0^{1.6} U_0^{0.8} \dots\dots\dots (6.3b)$$

In this case, the impact pressure relates to the thickness of the approaching landslide debris and can be substantially reduced for relatively ‘thin’ debris. The difference of F_A values obtained using the two approaches reduces substantially as the landslide debris becomes thicker.

Equations 6.3a and 6.3b can be related to the discharge rate of the landslide debris (Q_0) as shown in Equations 6.4a and 6.4b below:

$$F_A = \gamma \rho Q_0 U_0 \dots\dots\dots (6.4a)$$

$$F_A = 5 \rho g^{0.6} w^{0.2} h_0^{0.8} Q_0^{0.8} \dots\dots\dots (6.4b)$$

Much work has gone into improving the understanding of mechanisms of impact of snow avalanche on obstacles (Hákonardóttir, 2004) and design of snow avalanche protection measures (Jóhannesson et al, 2009). It can be noted that the pressure or reaction force on a barrier impacted by snow varies over the duration of impact. The relatively high dynamic pressure will usually last only a very short duration, and over the majority of the duration of deposition of material behind the barrier, the external load acting on the barrier is contributed mainly by static pressure of the deposit. Recognising the differences in material characteristics (e.g. compressibility and density) between snow and landslide debris, further work to understand the impact of landslide debris on landslide barrier is warranted for this assessment, which is currently being developed based on the assumption of ‘constant’ impact force/pressure over the duration of impact.

The rate of increase in volume of the debris deposited behind the barrier is related to the discharge rate of landslide debris (Q_0) by the following continuity equation:

$$V_D = Q_0 t \dots\dots\dots (6.5)$$

The net resistance provided by the landslide debris deposited behind the barrier at time t is given by the following equation (given that the forward moving velocity of the landslide debris is much greater than that of the flexible barrier over the duration since commencement of impact, t):

$$F_D = (\mu \cos \theta - \sin \theta) \rho g V_D = (\mu \cos \theta - \sin \theta) \rho g Q_0 t \dots\dots\dots (6.6)$$

A portion of the kinetic energy of the approaching landslide debris will become impact energy on the barrier. For a conservative estimate of the impact energy to be absorbed by the barrier, the internal strain energy of the debris mass between the barrier and the impacting landslide debris is ignored (i.e. the debris mass deposited behind the barrier is effectively assumed to be infinitely rigid). Assuming no loss of energy due to internal deformation of the landslide debris deposited behind the barrier on impact by the approaching debris, the rate of work done by the approaching debris (e_A) could be expressed by the following equation.

$$e_A = \frac{\rho Q_0 U_0^2}{2} = F_A \Delta_t \dots\dots\dots (6.7)$$

where Δ_t can be taken as rate of ‘virtual displacement’ associated with the work done generated by the impact force. The rate of ‘virtual displacement’ given in Equation (6.7) can also be obtained with reference to Equations 6.4a and 6.4b.

$$\Delta_t = \frac{e_A}{F_A} = \frac{\rho Q_0 U_0^2}{2 \gamma \rho Q_0 U_0} = \frac{U_0}{2\gamma} \dots\dots\dots (6.8a)$$

$$\Delta_t = \frac{e_A}{F_A} = \frac{\rho Q_0 U_0^2}{10 \rho g^{0.6} w^{0.2} h_0^{0.8} Q_0^{0.8}} \dots\dots\dots (6.8b)$$

The net reduction in kinetic energy due to basal friction minus the body force vector in the direction of the debris channel (e_D) is also related to rate of ‘virtual displacement’ as follows:

$$e_D = F_D \Delta_t = (\mu \cos \theta - \sin \theta) \rho g Q_0 t \Delta_t \dots\dots\dots (6.9)$$

By ignoring the strain energy of the debris mass deposited behind the barrier, the rate of change of kinetic energy (e_k) of the approaching ‘active’ landslide debris at any time t during the ‘effective’ impact period to be absorbed by the flexible barrier is given by combining Equations 6.7 to 6.9 as follows for the two considerations of impact force from the approaching landslide debris.

$$e_k = e_A - e_D = (F_A - F_D) \Delta_t = (\gamma \rho Q_0 U_0 - (\mu \cos \theta - \sin \theta) \rho g Q_0 t) \frac{U_0}{2\gamma} \dots\dots (6.10a)$$

$$e_k = e_A - e_D = (F_A - F_D) \Delta_t$$

$$= (5 \rho g^{0.6} w^{0.2} h_0^{0.8} Q_0^{0.8} - (\mu \cos \theta - \sin \theta) \rho g Q_0 t) \frac{\rho Q_0 U_0^2}{10 \rho g^{0.6} w^{0.2} h_0^{0.8} Q_0^{0.8}} \dots\dots (6.10b)$$

As noted above, the landslide debris mass deposited behind the barrier is conservatively taken to be infinitely rigid, and the loss of energy due to internal strain/deformation of the debris mass between the barrier and the impacting landslide debris is ignored.

For a conservative estimate of the impact energy to be absorbed by the barrier, the internal strain energy of the debris mass between the barrier and the impacting landslide debris is ignored (i.e. the stationary debris mass is effectively assumed to be rigid).

The ‘effective’ impact to the barrier is considered to be completed at time T_s when the net basal resistance mobilised (F_D) equals or exceeds the impacting force (F_A) of the approaching debris. This impact duration (T_s) can be determined using Equation 6.4a or 6.4b considering the two approaches in the assessment of impact pressure and Equation 6.6 above.

$$T_s = \frac{\gamma U_0}{(\mu \cos \theta - \sin \theta) g} \dots\dots\dots (6.11a)$$

or

$$T_s = \frac{(5 g^{0.6} h_0^{0.6} U_0^{-1.2}) U_0}{\mu g} = \frac{5 h_0^{0.6}}{(\mu \cos \theta - \sin \theta) g^{0.4} U_0^{0.2}} \dots\dots\dots (6.11b)$$

The duration of impact (T_s) is limited by the total active volume of landslide debris (V) given the discharge rate of landslide debris (Q_0) as follows:

$$T_s \leq \frac{V}{Q_0} \dots\dots\dots (6.12)$$

The kinetic energy to be absorbed by the debris flow barrier (E_B) in the whole impact process is obtained by integrating Equation 6.10 (viz. ignoring contribution of internal strain energy of the debris deposited behind the barrier) over the whole impact duration (T_s from Equation 6.11 and the duration limit T_s from Equation 6.12).

$$E_B = \int_0^{T_s} (\gamma \rho Q_0 U_0 - (\mu \cos \theta - \sin \theta) \rho g Q_0 t) \frac{U_0}{2\gamma} dt = \frac{\gamma \rho Q_0 U_0^3}{4 (\mu \cos \theta - \sin \theta) g} \dots (6.13a)$$

$$E_B = \int_0^{T_s} (5 \rho g^{0.6} w^{0.2} h_0^{0.8} Q_0^{0.8} - (\mu \cos \theta - \sin \theta) \rho g Q_0 t) \frac{\rho Q_0 U_0^2}{10 \rho g^{0.6} w^{0.2} h_0^{0.8} Q_0^{0.8}} dt$$

$$= \frac{5 \rho Q_0 h_0^{0.6} U_0^{1.8}}{4 (\mu \cos \theta - \sin \theta) g^{0.4}} \dots\dots\dots (6.13b)$$

It is useful to note that, the duration of impact as indicated in Equations 6.11a and 6.11b is independent of the total volume of landslide debris involved. Nevertheless, the energy to be absorbed by the barrier should be limited by the kinetic energy of the entire debris mass i.e. $E_B \leq \rho V U^2/2$. For the situation where $U_0 = 10$ m/s and $\phi = 15^\circ$, $T_s \approx 4$ sec is obtained for $\gamma = 1$ using Equation 6.11a or $h_0 = 0.6$ m using the approach suggested by Hübl et al (2009) in Equation 6.11b, which happens to be the same as that reported by Wartmann & Salzmann (2002).

The behaviour of the debris deposited behind the barrier under the impact of subsequent flow of debris can vary significantly. There are great uncertainties on internal friction angle as well as the basal friction between the landslide debris and the channel base, which can be between, say, $\phi = 35^\circ$ for fully drained granular material (under ‘static’ conditions), $\phi \approx 20^\circ$ for the same material under pore pressure for same ‘static’ condition but with a full hydrostatic groundwater level at the surface, and $\phi = 8^\circ$ to 11° under ‘dynamic’ conditions as adopted in landslide debris mobility models for debris flows in Hong Kong. For the range of $\phi = 8^\circ$ to 35° , assuming $\gamma = 1$ and $U_0 = 10$ m/s, T_s is found to vary between 1.5 seconds and 7 seconds using Equations 6.11a and 6.11b if h_0 remains unchanged at 0.6 m.

For scenarios where the debris channel behind the barrier is steep and the basal friction of the debris behind the barrier is small, the impact duration, T_s calculated based on equilibrium consideration will be very large. In case of long duration effective impact, the consideration of variation of impact pressure over the duration of impact and the loss of kinetic energy due to ‘inelastic’ impacts of landslide debris on debris deposited behind the barrier can become important. However, these considerations have been ignored in the assessment above.

6.2 Run-up Mechanism

Similar to the pile-up mechanism, the analysis adopts the Lagrangian approach and the frame of reference is the location of the flexible barrier, which moves forward under the impact pressure of the landslide debris. Assuming there is no change in discharge rate for the section of debris flow path interacting with the barrier ($dQ / dx = 0$; i.e. no deposition or entrainment), it can be demonstrated that the dissipation of kinetic energy of the landslide debris along its runout path on top of the debris deposited behind the barrier is due to the change in potential energy from its run-up height and frictional resistance mobilised on the debris flow path, as follows:

$$\frac{de_k}{dx} = -\rho g Q_0 (\sin(\theta) + \mu \cos(\theta)) \dots\dots\dots (6.14)$$

where θ = average inclination of the debris deposition behind the barrier (see Figure 5.1b).

Assuming the height of the deformed barrier upon impact is perpendicular to the ground surface and the forward moving velocity of the landslide debris is much greater than that of the flexible barrier over the duration since commencement of impact (t), the distance from the approaching landslide debris to the face of the barrier wall (X) can be obtained from consideration of continuity of the volume of debris deposition behind the barrier as follows:

$$X = \sqrt{\frac{2 U_0 h_0 t}{\tan(\theta + \alpha)}} \dots\dots\dots (6.15)$$

where α = average inclination of the debris movement path behind the barrier (see Figure 5.1b). Combining Equation 6.15 with the integral of Equation 6.13, the rate of change of kinetic energy of the landslide debris upon impact with the barrier (viz. the rate of kinetic energy to be absorbed by the flexible barrier, e_B , at time t) can be obtained:

$$e_B = e_0 - \rho g Q_0 (\sin(\theta) + \mu \cos(\theta)) \frac{1}{\cos(\theta + \alpha)} \sqrt{\frac{2 U_0 h_0 t}{\tan(\theta + \alpha)}} \dots\dots\dots (6.16)$$

where the kinetic energy of the approaching landslide debris is given by $e_0 = \frac{\rho Q_0 U_0^2}{2}$ for the condition of no entrainment/deposition.

Assuming the barrier is higher than the final run-up height (viz. H_D) of the landslide debris when the kinetic energy of the landslide debris reaching the face of the barrier wall reduces to zero ($e_B = 0$ in Equation 6.16), the duration of the ‘impact period’ can be determined (which is limited by the total active volume of the landslide) as follows:

$$T_s = \frac{U_0^3 \sin(\theta + \alpha) \cos(\theta + \alpha)}{8 h_0 g^2 (\sin(\theta) + \mu \cos(\theta))^2} \leq \frac{V}{Q_0} \dots\dots\dots (6.17)$$

and

$$H_D = \sqrt{2 U_0 h_0 T_s \tan(\theta + \alpha)} \dots\dots\dots (6.18)$$

For a retention barrier which has sufficient height against the highest run-up height of the landslide debris deposited behind the wall until the velocity of the debris on impact of the barrier becomes zero, the total kinetic energy of the landslide debris to be absorbed by the flexible barrier can be obtained by integrating Equation 6.16 over the ‘impact period’ with T_s as given by Equation 6.17 as follows:

$$E_B = \int_0^{T_s} \left(e_0 - \rho g Q_0 (\sin(\theta) + \mu \cos(\theta)) \frac{1}{\cos(\theta + \alpha)} \sqrt{\frac{2 U_0 h_0 t}{\tan(\theta + \alpha)}} \right) dt$$

$$= \frac{\rho Q_0 U_0^5 \cos(\theta + \alpha) \sin(\theta + \alpha)}{48 h_0 g^2 (\mu \cos(\theta) + \sin(\theta))^2} \leq \frac{\rho V U_0^2}{2} - \frac{(\mu \cos(\theta) + \sin(\theta)) \rho g \sin(\alpha + \theta)}{3} \sqrt{\left(\frac{8 h_0 U_0 V^3}{Q_0 \tan^3(\alpha + \theta)} \right)} \dots (6.19)$$

Equation 6.19 can be simplified conservatively by ignoring the basal friction resistance on the run-up ramp behind the wall by assigning $\mu = 0$:

$$E_B = \frac{\rho Q_0 U_0^5 \cos(\theta + \alpha) \sin(\theta + \alpha)}{48 h_0 g^2 \sin^2(\theta)} \leq \frac{\rho V U_0^2}{2} - \frac{(\sin(\theta)) \rho g \sin(\alpha + \theta)}{3} \sqrt{\left(\frac{8 h_0 U_0 V^3}{Q_0 \tan^3(\alpha + \theta)} \right)} \dots (6.20)$$

In this case, the duration of ‘impact period’ can also be obtained from Equation 6.17 assuming $\mu = 0$, as follows:

$$T_s = \frac{U_0^3 \sin(\theta + \alpha) \cos(\theta + \alpha)}{8 h_0 g^2 \sin^2(\theta)} \leq \frac{V}{Q_0} \dots\dots\dots (6.21)$$

If this method is to be adopted for design of barrier structures, judgement should be made whether the basal friction of the moving sheet of debris on the run-up ramp behind the wall should be taken as $\mu = 0$ as adopted for the basal friction of the debris deposited behind the barrier for the pile-up mechanism (see Section 6.1).

For a short check dam that requires a shorter time to fully fill up than the T_s calculated using Equation 6.21, the duration of the ‘impact period’ will be less than T_s given by Equation 6.21 and is related to the barrier height (H_B) as follows:

$$T_f = \frac{H_B^2}{2 U_0 h_0 \tan(\theta + \alpha)} \leq \frac{V}{Q_0} \dots\dots\dots (6.22)$$

In this case, the total kinetic energy of the landslide debris to be absorbed by the flexible barrier over the ‘impact period’ can be obtained by integrating Equation 6.16 with T_f given by Equation 6.22 and that it is not limited by V/Q_0 , as follows:

$$\begin{aligned}
 E_B &= \int_0^{T_f} (e_0 - \rho g Q_0 (\sin(\theta) + \mu \cos(\theta))) \frac{1}{\cos(\theta + \alpha)} \sqrt{\frac{2 U_0 h_0 t}{\tan(\theta + \alpha)}} dt \\
 &= \frac{\rho Q_0 U_0 H_B^2}{4 h_0 \tan(\theta + \alpha)} - \frac{\rho g Q_0 H_B^3}{3 h_0 U_0 \tan(\theta + \alpha) \sin(\theta + \alpha)} (\sin(\theta) + \mu \cos(\theta)) \dots\dots\dots (6.23)
 \end{aligned}$$

Equation 6.23 can also be simplified conservatively by ignoring the frictional interaction in the debris run-up process as follows:

$$E_B = \frac{\rho Q_0 H_B^2}{h_0 \tan(\theta + \alpha)} \left(\frac{U_0}{4} - \frac{g H_B \sin(\theta)}{3 U_0 \sin(\theta + \alpha)} \right) \dots\dots\dots (6.24)$$

It should be noted that the design height of barrier is not solely governed by the run-up height of the debris. In particular, the design retention capacity of the barrier and the amount of height reduction due to barrier deformation upon impact may also affect the design height of the barrier.

When the landslide debris overspills the top rope of the barrier, the top edge of the barrier fence will be subjected to further drag forces in addition to the kinetic energy of the landslide debris on direct impact with the barrier assessed using Equations 6.23 and 6.24.

Table 6.1 summaries the kinetic energy of the landslide debris to be absorbed by a flexible barrier for the different simplified deposition mechanisms and scenarios considered. It may be necessary for designers to assess the design of flexible barriers against landslide impact and check the different mechanisms and scenarios proposed.

Worked examples illustrating the approaches using the existing methods, together with the proposed approaches for assessing the energy absorption requirement of a flexible barrier impacted by landslide debris for different design scenarios, are presented in Appendix A.

It is pertinent to note from the examples presented in Section A.2 that the assumption of basal friction for the moving sheet of debris on the run-up ramp behind the barrier is very sensitive to the assessment assuming a run-up mechanism. For a moderate (and conservative) friction angle of 11°, the calculated duration of impact and energy rating of the barrier are much reduced when compared with that calculated based on the assumption of no basal friction on the run-up ramp. If this is the case, the pile-up mechanism might possibly be the principal controlling scenario in the sizing of flexible barriers for ‘typical’ natural terrain landslides in Hong Kong. However, this preliminary observation would need to be reviewed.

Table 6.1 Analytical Solutions for Impact of Landslide Debris on Flexible Barriers

Deposition Mechanism and Scenario	Design Impact Energy of Barrier (E_B)	Duration of Impact (T), with $T_s \leq \frac{V}{Q_0}$
Pile-up mechanism: Impact pressure according to Lo (2000)	$E_B = \frac{\gamma \rho Q_0 U_0^3}{4 (\mu \cos \theta - \sin \theta) g}$	$T_s = \frac{\gamma U_0}{(\mu \cos \theta - \sin \theta) g}$
Pile-up mechanism: Impact pressure according to Hübl et al (2009)	$E_B = \frac{5 \rho Q_0 h_0^{0.6} U_0^{1.8}}{4 (\mu \cos \theta - \sin \theta) g^{0.4}}$	$T_s = \frac{5 h_0^{0.6}}{(\mu \cos \theta - \sin \theta) g^{0.4} U_0^{0.2}}$
Run-up mechanism: ($H_B \geq H_D$)	$E_B = \frac{\rho Q_0 U_0^5 \cos(\theta + \alpha) \sin(\theta + \alpha)}{48 h_0 g^2 (\mu \cos \theta + \sin \theta)^2}$	$T_s = \frac{U_0^3 \sin(\theta + \alpha) \cos(\theta + \alpha)}{8 h_0 g^2 (\sin \theta + \mu \cos \theta)^2}$
Run-up mechanism: ($H_B \geq H_D$) $\mu = 0$	$E_B = \frac{\rho Q_0 U_0^5 \cos(\theta + \alpha) \sin(\theta + \alpha)}{48 h_0 g^2 \sin^2(\theta)}$	$T_s = \frac{U_0^3 \sin(\theta + \alpha) \cos(\theta + \alpha)}{8 h_0 g^2 \sin^2(\theta)}$
Run-up mechanism: ($H_B < H_D$)	$E_B = \frac{\rho Q_0 U_0 H_B^2}{4 h_0 \tan(\theta + \alpha)} - \frac{\rho g Q_0 H_B^3}{3 h_0 U_0 \tan(\theta + \alpha) \sin(\theta + \alpha)} (\sin(\theta) + \mu \cos(\theta))$	$T_f = \frac{H_B^2}{2 U_0 h_0 \tan(\theta + \alpha)}$
Run-up mechanism: ($H_B < H_D$) $\mu = 0$	$E_B = \frac{\rho Q_0 H_B^2}{h_0 \tan(\theta + \alpha)} \left[\frac{U_0}{4} - \frac{g H_B \sin(\theta)}{3 U_0 \sin(\theta + \alpha)} \right]$	

Nevertheless, the energy rating of the flexible barrier required for mitigation of landslides is most sensitive to velocity of the debris movement. Given the currently commercially available ‘strongest’ flexible barrier sized using energy rating, it may have rather limited capacity in mitigation of landslide impacts (e.g. in the order of a 300 m³ landslide travelling at a speed of about 11 m/s).

7 Debris-barrier Interaction

Analyses presented in Section 6 above incorporate consideration of largely the kinetic energy of the frontal portion of the landslide debris, with no explicit account taken of the reaction and interaction of the barrier, as well as the debris deposited behind the barrier. Loss of kinetic energy due to inelastic impact of the landslide debris as well as variation of impact pressure over the duration of impact have not been incorporated in the simplified (and conservative) analytical model, in view of the complexity and uncertainties involved.

In this Section, a preliminary assessment framework for the overall interaction of debris impact on flexible barrier is discussed. Upon impact by landslide debris, the flexible barrier resists movement of the approaching debris and retains the landslide debris deposited behind it by exerting a reaction force to the debris. By incorporating the characteristics of the (dynamic) response of the flexible barrier under impact, the interaction between the approaching debris and the flexible barrier can be examined in greater detail, and probably in a more realistic manner.

7.1 Characterisation of Barrier Responses

An external force (F_b) acting on the flexible barrier generates deflection (Δ) of the barrier as well as energy absorption, which comprises storage of elastic strain energy and energy loss due to plastic deformation of the barrier, and with time impact energy absorbed by debris deposited behind the barrier. The structural responses of the barrier to the applied external force can be represented by the characteristics between external force (F_b) and deformation (Δ), as well as the impact energy to be absorbed by the barrier (E_t), as follows:

$$F_b = f(\Delta) = f(E_t) \dots\dots\dots (7.1)$$

The impact energy to be taken up (absorbed) by the barrier at any time t during the impact is the sum of the work done by the reaction force and the energy loss due to inelastic deformation of the barrier as well as the debris deposited behind it:

$$E_t = \int (F_u \times U - E_f, t) \dots\dots\dots (7.2)$$

To evaluate the energy loss due to inelastic deformation of the barrier and the debris deposited behind the barrier, the conventional approach in structural dynamics is to incorporate a damping force (F_f), as follows:

$$E_f = F_f \times U \dots\dots\dots (7.3)$$

The effect of damping is associated with a dissipative process during deformation such as frictional loss. Damping of the flexible barrier and the debris deposited behind it under the impact of the approaching landslide debris is complex. Subject to further studies, probably the simplest assumption for overall damping behaviour is to adopt a viscous model:

$$F_f = C \times U \dots\dots\dots (7.4)$$

where C is the viscous damping coefficient, and in case of debris impact on flexible barrier, it represents the damping effect of the barrier and the debris deposited behind it.

7.2 Balance of Forces and Barrier Deflection

For overall balance of forces, the impact force (F_a) exerted by the approaching debris is to be resisted by the reaction force by the barrier (F_B) and the net resistance (F_D) of the landslide debris deposited behind the barrier, which is similar to the dynamic analysis of the pile-up deposition of debris behind the barrier (Section 6.1). The net force (in the direction of the flow of the landslide debris), viz. the unbalanced force (F_u), is given as follows:

$$F_u = F_a - F_D - F_B - F_f \dots\dots\dots (7.5)$$

where F_f is the viscous damping arising from energy loss due to inelastic deformation as discussed in Section 7.1 above.

Out of balance forces will generate acceleration and deflection of the barrier, as given below:

$$\frac{dU}{dt} = \frac{F_u}{(m_b + m_d)} \dots\dots\dots (7.6)$$

where m_b is the mass of the barrier and m_d is the effective mass of the debris deposited behind it. The reaction force of the barrier (F_b) is related to the deflection of the barrier which can be fed into the equilibrium equation above.

The impact pressure by debris approaching landslide debris is eventually balanced by the combined resistance from the deposit and the deflected barrier. Through the barrier characteristics, the build-up of impact energy to be absorbed by the barrier can also be assessed.

As discussed in Section 6.1 above, the high dynamic pressure of landslide debris may last for only a very short duration and over the majority of the duration of impact as an analogy to snow avalanche impact. Further work to improve the understanding of the impact of landslide debris on landslide barrier would be useful for further development of a more realistic assessment. The method of assessment developed so far has been based on the assumption of constant impact force/pressure over the duration of impact, which is conservative.

8 Discussions

The impact of multi-phase landslide debris (comprising solid particles, water and air) on a landslide-resisting barrier can involve very complex dynamic interaction of all the components of concern. A study of this complex problem requires simplification and assumptions that should capture, as far as possible, the key physical controlling factors and boundary conditions. In this preliminary study, the results of an attempt to diagnose the interaction mechanisms involved in the impact of landslide debris of different characteristics on flexible landslide-resisting barriers are presented. An initial quantitative assessment of the possible level of kinetic energy of the portion of landslide debris involved in the impact on the barrier for the different deposition mechanisms has been made.

Under the impact of landslide debris, a flexible barrier would deform and the further potential energy of the debris mass released (as compared with the initial elevation of the barrier) has not been accounted for explicitly in the present analysis. It is noted that the energy approach adopted in the sizing of flexible rockfall barriers considers the kinetic energy of the impacting boulder at the initial position of the barrier, and the potential energy released from the boulder and the deforming barrier subsequent to impact have been allowed for in the structural design of the barrier and verified in field tests. However, the potential differences in structural performance of a flexible barrier and its interaction with landslide debris when compared with that of a boulder fence conventionally sized according to energy levels of impacting boulders should not be ignored. It would be prudent to address the uncertainty in the performance of the structure if the impact energy rating of a rockfall fence is to be adopted for the same barrier under the impact of landslide debris.

It is noteworthy that the analytical solutions of debris impact energy developed and presented in this preliminary study involve various assumptions and simplifications. For example, the two deposition mechanisms may occur in an event when the barrier is hit by landslide debris of varying movement characteristics in different surges. There may be further run-up of landslide debris hitting the barrier after the time of impact as calculated assuming a pile-up mechanism. The pile-up mechanism also involves an assumption that the debris deposited behind the barrier is able to form a 'lumped mass' to resist further impact loading via friction mobilised at its base. In practice, unconsolidated debris would not necessarily behave as assumed and may not be as effective in 'protecting' the barrier as assumed. On the other hand, the approach would have some degree of conservatism as energy loss due to inelastic deformation of the debris on impact has been ignored and the high dynamic pressure of the landslide debris has been taken as being constant over the duration of impact. There may also be some 'residual' capacity of the steel mesh fence in retaining the debris deposited behind it after the calculated time of impact (*viz.* after the fence has been taken as having completely absorbed the energy of the impacting landslide debris). There are still great uncertainties in various aspects of the dynamic interaction between the landslide debris and the flexible barrier.

The assessment framework and the analytical solutions developed for the different scenarios and landslide debris movement characteristics in this preliminary study serve as a starting point in tackling this complex interaction problem, which may be taken forward further with suitable refinements with a view to formulating a rational and suitably robust design framework, with suitable allowance for uncertainty, perhaps for moderate landslides in Hong Kong or when the flexible barriers are used in conjunction with other mitigation measures (e.g. baffles reduce impact velocity of the landslide debris or facilities to ensure drainage of the landslide debris deposited behind the barriers).

The assessment developed in this preliminary study may help designers to gain a better appreciation of the possible deposition mechanisms of landslide debris behind a barrier as well as possible dynamic interaction between a flexible barrier and the landslide debris upon impact. For further technical development, the approaches presented here may help to support further work to arrive at a more fundamental understanding of the complex dynamic response of landslide debris upon impact on an obstacle (e.g. flexible barrier, baffle, etc.) through analytical, numerical and experimental methods.

Discussion of a preliminary assessment framework for the overall interaction of debris impact on flexible barrier has been presented. By incorporating the dynamic characteristics of the response of a flexible barrier, the interaction between the approaching debris and the flexible barrier can be examined in greater detail, and probably in a more realistic manner. The build-up of internal stresses within the barrier, as well as internal strain energy mobilised as the barrier is hit by the approaching debris and boulders (in terms of impact energy input) can be examined. It can be demonstrated from this assessment that loss of kinetic energy upon impact due to inelastic deformation of the barrier, as well as the debris deposited behind the barrier, can make a significant change to the 'actual' impact loading (or energy) to the barrier. Furthermore, the assumption of a constant 'high' dynamic pressure of the landslide debris over the duration of impact will likely provide a conservative estimate. Improved knowledge and better understanding in this area would help to reduce the uncertainty in the expected performance of barriers. In this regard, further work is warranted to examine the impact and interaction mechanisms (e.g. using other numerical models and/or physical model

tests), as well as benchmarking with the design of a wider range of barrier structures based on different approaches.

Appendix B presents a comparison of the analytical solutions with time-march finite difference calculations based on the same sets of differential equations for the various scenarios considered previously. This comparison provides a check on the analytical solutions as well as demonstrates the applicability of the approach using finite difference calculations, which can be adapted to incorporate site-specific consideration of the variations in velocity and flow depth of the impacting debris as well as local variations in the channel section. Given further work to clarify the uncertainty and gain more confidence in these assessments, the results from debris mobility modelling (e.g. parameters U , Q , h and w at different time-steps when the frontal portion of the landslide debris reaches the location of the barrier) may also be used in a more detailed assessment using finite difference calculations. In most of the numerical models/codes for landslide debris mobility modelling, the debris-barrier interaction (e.g. piling up of material behind the wall or the backward thickening of the approaching debris) could not be adequately represented. In view of the uncertainties involved, it would be prudent to adopt a more conservative approach, with suitably robust assumptions on debris velocity, influx and thickness values based on debris mobility models.

9 Conclusions

Based on observations in field and laboratory tests and with the support of numerical modelling (using the distinct element code PFC^{3D}), a preliminary assessment of the landslide deposition mechanisms involved in the impact of landslide debris on a flexible barrier (commonly comprising tensioned steel wire mesh) has been made in this preliminary study. For two different types of landslide debris with movement characteristics represented by means of viscous and frictional models, two possible deposition mechanisms are distinguished. These findings may form a basis for further work in formulating a rational and suitably robust methodology for sizing and designing debris-resisting flexible barriers, perhaps for moderate landslides in Hong Kong or when flexible barriers are used in conjunction with other mitigation measures. The assessments presented in this report may also help designers to gain a better appreciation of possible dynamic interaction between a flexible barrier and landslide debris upon impact.

For each of these two debris deposition mechanisms, the governing differential equations as well as analytical solutions for the duration of impact and kinetic energy to be absorbed by a flexible barrier have been developed based on some simplifying assumptions. These equations and solutions, whilst being only approximations, provide a starting point for a better understanding of the key factors that may have a bearing on the performance of a flexible barrier. With further development, consideration may be given to adopting these differential equations for use in finite difference calculations to take account of variations in debris flow velocity and discharge characteristics, which could be obtained from landslide debris mobility numerical models.

A preliminary assessment of the overall debris-barrier interaction indicates that loss of kinetic energy upon impact due to inelastic deformation of the barrier and variation of dynamic impact pressure over the duration of impact can make a significant influence to the

loading conditions on the barrier. Further work to examine the debris impact and interaction mechanisms and to reduce uncertainty in design assessments of barriers is warranted.

10 References

- Cundall, P.A. & Strack, O.D.L. (1979). A Discrete Numerical Model for Granular Assemblies. *Geotechnique*, vol. 29, issue 1, pp 47-65.
- Duffy, J.D. (2008). Debris flow mitigation using flexible barriers, prepared for the 59th Highway Geology Symposium, *Geobruigg Technical Documentation*, June 2008.
- Grassl, H., Volkwein, A., Anderheggen, E. & Ammann, W.J. (2002). Steel-net rockfall protection - experimental and numerical simulation, *Structures Under Shock and Impact VII*, pp 143-153.
- Hákonardóttir, K.M. (2004). *The Interaction between Snow Avalanches and Dams*. University of Bristol, PhD Thesis, 142 p.
- Hübl, J., Suda, J., Proske, D., Kaitna, R. & Scheidl, C. (2009). Debris flow impact estimation. *Proc. of the 11th Int. Sym. on Water Management and Hydraulic Engineering*, Macedonia, pp 139-148.
- Itasca (2005). *Particle Flow Code in 3 Dimensions*. Itasca Consulting Group Inc.
- Jóhannesson, T., Gauer, P., Issler, P. & Lied, K. (2009). *The Design of Avalanche Protection Dams - Recent Practical and Theoretical Developments*, Directorate-General for Research, Environment Directorate, European Commission, EUR2339, 205 p.
- Law, R.P.H., Zhou G.D., Chan Y.M. & Ng C.W.W. (2007). Investigations of fundamental mechanisms of dry granular debris flow. *Proc. 16th Southeast Asia Geot. Conf.* 8-11 May, Malaysia: pp 781-786.
- Law R.P.H. (2008). *Investigations of Mobility and Impact Behaviour of Granular Flows*. MPhil Thesis of Hong Kong University of Science and Technology, 378 p.
- Lo, D.O.K. (2000). *Review of Natural Terrain Landslide Debris-resisting Barrier Design*, *GEO Report No. 104*. Geotechnical Engineering Office, Hong Kong, 91 p.
- Mancarella, D. & Hungr, O. (2010). Analysis of run-up of granular avalanches against steep, adverse slopes and protective barriers. *Canadian Geotechnical Journal*, vol. 47, pp 827-841.
- Roth, A., Kästli, A. & Frenez, T. (2004). Debris flow mitigation by means of flexible barriers. *Internationales Symposium Interpraevent 2004 – Riva / Trient*, vol. VII, pp 289-300.

- Shum, L.K.W., Lam, A.Y.T., Kwan, J.S.H. & Koo, R.C.H. (2011). *An Overview on the Use of Flexible Barriers in Mitigating Natural Terrain Landslides, Discussion Note No. DN 1/2011*, Geotechnical Engineering Office, Hong Kong, 82 p.
- Wartmann, St. & Salzmänn, H. (2002). Debris flow and floating tree impacts on flexible barriers. *Natural Terrain - A Constraint to Development?* The Institution of Mining and Metallurgy - Hong Kong Branch, pp 125-131.
- Wendeler, C., Bartelt, P. & Salzmänn, H. (2010). *Structural Design of Flexible Steel Barriers for Torrent Debris Flow Mitigation* (paper submitted to Landslides Journal for publication).

Appendix A
Worked Examples

Contents

	Page No.
Cover Page	34
Contents	35
A.1 Example 1 - Debris Flow Impacting on a Flexible Barrier - Using Existing Methods of Assessment	36
A.2 Example 2 - Debris Flow Impacting on a Flexible Barrier	37

A.1 Example 1 - Debris Flow Impacting on a Flexible Barrier - Using Existing Methods of Assessment

Given

1. The design landslide event is a debris flow.
2. The transportation zone is steeply inclined resulting in a relatively high approaching velocity.
3. A flexible debris flow barrier is proposed to be installed downstream of the flow path to retain the landslide debris.
4. The design data of the design debris flow event are shown below:

Table A1

Design Data	
Design volume	300 m ³
Bulk density	1.8 Mg/m ³
Approaching velocity	9 m/s
Discharge rate	13.5 m ³ /s
Flow depth	0.5 m

Tasks

1. Calculate the runup height of the debris for sizing of the barrier.
2. Calculate the required energy absorption capacity of the flexible barrier using the lumped mass model assuming the barrier is required to absorb the kinetic energy of the entire debris mass.
3. Calculate the required energy absorption capacity of the flexible barrier using Wartmann & Salzmann (2002) method using the debris velocity and discharge rate given above and assuming the duration of interaction between the barrier and the debris mass is 4 seconds.
4. It should be noted that the sizing of the barrier using the above approaches does not require the consideration of the basal friction of debris deposited behind the barrier.

Run-up height

For the barrier to retain the impacting debris, it is necessary for the barrier to have a sufficient height when compared with the maximum vertical run-up distance of the landslide debris, which may be estimated based on conservation of energy as follows:

$$H_D = \frac{U_0^2}{2g} = 4.1 \text{ m}$$

Energy absorption capacity

Energy absorption capacity of the flexible barrier using the lumped mass model assuming the barrier is required to absorb kinetic energy of the entire debris mass:

$$E_B = \frac{mU^2}{2} = \frac{300 \text{ m}^3 \times (9 \text{ ms}^{-1})^2}{2} = 12,150 \text{ kJ}$$

Energy absorption capacity required based Wartmann & Salzmann (2002) method using the debris velocity and discharge rate given in Table A1:

$$E_B = \frac{m_a U^2}{2} = \frac{\rho Q T_s U^2}{2} = \frac{1.8 \text{ Mgm}^{-3} \times 13.5 \text{ m}^3 \text{ s}^{-1} \times 4 \text{ s} \times (9 \text{ ms}^{-1})^2}{2} = 3,936 \text{ kJ}$$

A.2 Example 2 - Debris Flow Impacting on a Flexible Barrier

Given

1. The design landslide event is a debris flow.
2. The transportation zone is steeply inclined resulting in a relatively high approaching velocity.
3. A flexible debris flow barrier is proposed to be installed downstream of the flow path in order to retain the landslide debris.
4. Design data of the design debris flow event are shown below:

Table A2

Design Data	
Design volume	300 m ³
Bulk density	1.8 Mg/m ³
Approaching velocity	9 m/s
Discharge rate	13.5 m ³ /s
Flow depth	0.5 m
Basal friction	11°
Inclination of the landslide deposit	11°
Inclination of landslide debris flow path	0°

Tasks

1. Calculate the impact duration for direct interaction with the flexible barrier.
2. Calculate the required energy absorption capacity of the flexible barrier.
3. Calculate run-up height of the debris for sizing of the barrier.

Approach

The landslide debris may involve pile-up or run-up mechanisms behind the flexible barrier during impact. Therefore, it would be prudent to assess the energy absorption capacity of the flexible barrier for the two possible deposition mechanisms concerned.

Pile-up mechanism

The impact duration of (T_s) which is assessed using Equation 6.11b. Following the approach on assessment of impact pressure recommended by Lo (2000), but considering the impact of landslide debris on a flexible barrier or a deformable block of debris, a dynamic pressure coefficient of unity is adopted.

$$T_s = \frac{\gamma U_0}{(\mu \cos \theta - \sin \theta) g} = \frac{9 \text{ ms}^{-1}}{(\tan(11^\circ) \times \cos(0^\circ) - \sin(0^\circ)) \times 9.81 \text{ ms}^{-2}} = 4.7 \text{ s}$$

The calculation of the required energy absorption capacity of the flexible debris flow barrier (E_B) follows Equation 6.10a and with a load factor of unity.

$$E_B = \frac{\rho Q_0 U_0^3}{4 (\mu \cos \theta - \sin \theta) g} = \frac{1.8 \text{ Mgm}^{-3} \times 13.5 \text{ m}^3 \text{s}^{-1} \times (9 \text{ ms}^{-1})^3}{4 \times (\tan(11^\circ) \cos(0^\circ) - \cos(0^\circ)) \times 9.81 \text{ ms}^{-2}} = 2,323 \text{ kJ}$$

Run-up mechanism

The calculation of the impact duration (T_s) follows Equation 6.17.

$$T_s = \frac{U_0^3 \sin(\theta + \alpha) \cos(\theta + \alpha)}{8 h_0 g^2 (\sin(\theta) + \mu \cos(\theta))^2}$$

$$= \frac{(9 \text{ ms}^{-1})^3 \times \sin(11^\circ + 0^\circ) \times \cos(11^\circ + 0^\circ)}{8 \times 0.5 \text{ m} \times (9.81 \text{ ms}^{-2})^2 \times (\sin(11^\circ) + \tan(11^\circ) \times \cos(11^\circ))^2} = 2.4 \text{ s}$$

and is less than $V/Q_0 = 300 \text{ m}^3 / 13.5 \text{ m}^3/\text{s} = 22.2 \text{ s}$

The calculation of the required energy absorption capacity of the flexible debris flow barrier (E_B) by ignoring the basal friction of the impacting landslide debris on its run-up ramp and follows Equation 6.19, which could also be found in Table 6.1.

$$E_B = \frac{\rho Q_0 U_0^5 \cos(\theta + \alpha) \sin(\theta + \alpha)}{48 h_0 g^2 (\mu \cos \theta + \sin \theta)^2}$$

$$= \frac{1.8 \text{ Mgm}^{-3} \times 13.5 \text{ m}^3\text{s}^{-1} \times (9 \text{ ms}^{-1})^5 \times \sin(11^\circ + 0^\circ) \times \cos(11^\circ + 0^\circ)}{48 \times 0.5 \text{ m} \times (9.81 \text{ ms}^{-2})^2 \times (\sin(11^\circ) + \tan(11^\circ) \times \cos(11^\circ))^2} = 799 \text{ kJ}$$

In consideration of the possible pile-up and run-up deposition mechanisms involved in the impact of landslide debris behind the barrier, it would be prudent to adopt the higher value of calculated E_B (viz. 2,323 kJ, or rounded up to 3,000 kJ) for the flexible barrier to be provided.

It would also be useful to compare the calculation assuming that the basal friction of the moving sheet of debris on the run-up ramp behind the wall is taken as $\mu = 0$ and calculation of the impact duration (T_s) follows Equation 6.21.

$$T_s = \frac{U_0^3 \sin(\theta + \alpha) \cos(\theta + \alpha)}{8 g^2 h_0 \sin^2 \theta} = \frac{(9 \text{ ms}^{-1})^3 \times \sin(11^\circ + 0^\circ) \times \cos(11^\circ + 0^\circ)}{8 \times (9.81 \text{ ms}^{-2})^2 \times 0.5 \text{ m} \times \sin(11^\circ)^2} = 9.7 \text{ s}$$

and is less than $V/Q_0 = 300 \text{ m}^3 / 13.5 \text{ m}^3/\text{s} = 22.2 \text{ s}$

In this case, the calculation of the required energy absorption capacity of the flexible debris flow barrier (E_B) by ignoring the basal friction of the impacting landslide debris on its run-up ramp and follows Equation 6.20, which could also be found in Table 6.1.

$$E_B = \frac{\rho Q_0 U_0^5 \cos(\theta + \alpha) \sin(\theta + \alpha)}{48 h_0 g^2 \sin^2(\theta)}$$

$$= \frac{1.8 \text{ Mgm}^{-3} \times 13.5 \text{ m}^3\text{s}^{-1} \times (9 \text{ ms}^{-1})^5 \times \sin(11^\circ + 0^\circ) \times \cos(11^\circ + 0^\circ)}{48 \times 0.5 \text{ m} \times (9.81 \text{ ms}^{-2})^2 \times \sin^2(11^\circ)} = 3,196 \text{ kJ}$$

With the simplification of $\mu = 0$, the calculated the time of impact as well as impact the energy to be absorbed by the barrier before significantly greater that the with the assessment adopting $\mu = 11^\circ$, which is consistent with the basal friction adopted for the pile-up mechanism.

It may be noted that the above assessment is sensitive to the assumptions made (e.g. mobilisation of frictional resistance on the run-up ramp) and the parameters adopted (e.g. $\tan^{-1}\mu$: the friction angle mobilised at the base of the debris mass piled up behind the barrier, and θ : the inclination of debris deposition behind the barrier forming a run-up ramp). Given the uncertainty in field behaviour of the landslide debris as well as the performance of the barrier structure in practice, it would be prudent to adopt suitably conservative assumptions at this stage of development and understanding. For example the parameters $\tan^{-1}\mu$ and θ can be taken as the interface friction angle being equal to the friction angle component of the Voellmy model parameters adopted in debris mobility analyses.

Run-up height

For the barrier to retain the impacting debris, it is necessary for the barrier to have a sufficient height when compared with the maximum vertical run-up distance of the landslide debris with consideration of conservation of energy as follows:

$$H_D = \frac{U_0^2}{2g} = 4.1 \text{ m}$$

Alternatively, the calculation of the effective height of the flexible debris flow barrier can also be assessed based on the height of the run-up ramp of the landslide debris deposit at the time where the impact process is considered complete and is given by Equation 6.18.

For basal friction angle of 0° , the impact time for run-up mechanism is 9.7 seconds and

$$H_D = \sqrt{2 U_0 h_0 T_s \tan(\theta + \alpha)} = \sqrt{2 \times 9 \text{ ms}^{-1} \times 0.5 \text{ m} \times 9.7 \text{ s} \times \tan(11^\circ + 0^\circ)} = 4.1 \text{ m}$$

For basal friction angle of 11° , the impact time is reduced to 2.4 seconds and

$$H_D = \sqrt{2 U_0 h_0 T_s \tan(\theta + \alpha)} = \sqrt{2 \times 9 \text{ ms}^{-1} \times 0.5 \text{ m} \times 2.4 \text{ s} \times \tan(11^\circ + 0^\circ)} = 2.0 \text{ m}$$

It will be prudent to provide a barrier of sufficient height to cover the maximum vertical run-up distance of at least 4.1 m.

Appendix B

Comparison between Analytical Solutions and Finite Difference Calculations for Debris-barrier Interaction Mechanisms

Contents

	Page No.
Cover Page	41
Contents	42
List of Tables	43
B.1 Introduction	44
B.2 Pile-up mechanism	44
B.3 Run-up mechanism	45
B.4 Results and Discussion	45

List of Tables

Table No.		Page No.
B1	Comparison of Analytical and Numerical Solutions for Pile-up Mechanism	46
B2	Comparison of the Analytical and Numerical Solutions for Run-up Mechanism	47

B.1 Introduction

Analytical solutions for both the pile-up and run-up mechanisms, as summarised in Table 6.1 are compared with the impact duration and kinetic energy of the landslide debris during the impact period calculated using a time-marching finite difference solution scheme. Both the analytical and finite difference calculations adopt the same set of governing differential equations. To simplify the calculations, the debris movement channel bed behind the barrier is taken to be horizontal and the interface friction between the approaching landslide debris and the deposit in the run-up mechanism is taken to be the same as the friction angle mobilised for the landslide debris deposited behind the barrier in the pile-up mechanism.

B.2 Pile-up mechanism

The duration of landslide debris impacting on a flexible barrier is divided into numerous time steps and the basal friction angle of the landslide debris deposited behind the barrier is considered to be constant within each time step. In each time step, the volume of landslide debris deposited behind the barrier is calculated as follows:

$$V_{D\Delta T} = Q_0 \Delta t \dots\dots\dots (B.1)$$

The basal frictional resistance of the landslide deposit is calculated using Equation 6.6.

The lateral compaction force acting on the landslide debris deposit behind the barrier by the approaching debris (F_A) can be calculated using Equations 6.4a and 6.4b. Adopting Equation 6.4a with dynamic pressure coefficient $\gamma = 1$, the compaction force can be simplified as follows:

$$F_A = \rho Q_0 U_0 \dots\dots\dots (B.2)$$

With reference to Equation 6.7 and ignoring the contribution from deformation of the landslide debris deposit, the kinetic energy to be absorbed by the flexible barrier ($\Delta E_{k\Delta T}$) in each time step is calculated using the following relationship:

$$\Delta E_{k\Delta T} = \frac{(\rho Q_0 U_0 - \mu \rho g Q_0 t) U_0 \Delta t}{2} \dots\dots\dots (B.3)$$

where Δt is the size of the time step adopted in the finite difference solution. The total kinetic energy to be absorbed by the flexible barrier is calculated by summing the $\Delta E_{k\Delta T}$ throughout the impact duration. As Q_0 and U_0 are constant throughout the impact period, at any time t , the kinetic energy to be absorbed by the flexible barrier is as follows:

$$E_k = \frac{\rho Q_0 U_0^2 t}{2} - \frac{\mu \rho g Q_0 U_0 t^2}{4} \dots\dots\dots (B.4)$$

The impact process is considered to be completed when the basal frictional resistance exceeds the impact force acting on the landslide deposit.

B.3 Run-up mechanism

Similarly, the calculation in this case starts with dividing the duration of landslide debris impacting on a flexible barrier into numerous time steps within which both the impacting velocity and the volume of the run-up ramp increase. At any time t , the height of the landslide debris deposited behind the flexible barrier is computed considering conservation of the volume of the approaching landslide debris and assuming a constant width of the channel/debris mass deposited behind the barrier as follows:

$$h_t = \sqrt{2 U_0 h_0 \tan(\theta + \alpha) t} \dots\dots\dots (B.5)$$

The velocity (U_t) of the landslide debris upon impact with the flexible barrier at time t , can then be computed with the consideration of velocity reduction due to change in potential energy from its run-up height and assuming no frictional loss along the run-up path as follows:

$$U_t = \sqrt{U_0^2 - 2 g \sqrt{(2 U_0 h_0 \tan(\theta + \alpha) t)} \left(1 + \frac{\mu}{\tan(\theta + \alpha)}\right)} \dots\dots\dots (B.6)$$

The kinetic energy to be absorbed by the flexible barrier ($\Delta E_{k\Delta T}$) in each time step is calculated using the following relationship:

$$\Delta E_{k\Delta T} = \frac{\rho Q_0 U_t^2 \Delta t}{2} \dots\dots\dots (B.7)$$

where Δt is the time step adopted in the finite difference solution. The total kinetic energy to be absorbed by the flexible barrier is calculated by summing $\Delta E_{k\Delta T}$ throughout the impact duration. The impact process is considered to be completed when $\Delta E_{k\Delta T}$ approaches zero (i.e. converted to potential energy in the run-up process).

The kinetic energy to be absorbed by the barrier is obtained by summing up by summing the $\Delta E_{k\Delta T}$ throughout the impact duration.

B.4 Results and Discussion

Tables B1 and B2 show the calculation steps and results of the kinetic energy to be absorbed by a flexible barrier using both the analytical solution and the time-marching finite difference scheme. It is observed from Tables B1 and B2 that the computed impact energy of the landslide debris on a flexible barrier using the finite difference approach matches closely with the one calculated using Equation 6.13a assuming load factor $\gamma = 1$ and Equation 6.20. The finite difference approach is a useful tool for calculating the impact energy and can be easily adapted to incorporate output from debris mobility models such that variations in approaching velocity (U_0) and the flow depth (h_0) and width (w) can be accommodated.

Table B1 Comparison of Analytical and Numerical Solutions for Pile-up Mechanism

Input parameters for finite difference calculations	
Time increment	0.2 s
Total volume of landside debris	300 m ³
Mass density of landside debris (ρ)	1800 kg/m ³
Discharge rate of landside debris (Q ₀)	13.5 m ³ /sec
Velocity of approaching landside debris (U ₀)	9 m/sec
Basal friction of landside debris deposit (φ)	11 °
Gravitational acceleration (g)	9.81 m/s ²

Notes:

[A] The time for each calculation step is the time of the previous step plus the time increment.

[B] Volume of debris deposited behind the barrier is calculated using Equation (B1) and is ≤ total volume of landside debris.

[C] Mass of debris deposited behind the barrier = [B] × ρ

[D] Basal resistance = [C] × g × tan (φ), as given in Equation (8).

[E] Compaction force, F_A, of approaching debris is calculated using Equation (B2) using U₀, and ρ given above.

[F] Kinetic energy of the landslide mass involved in impact E_k is calculated using Equation (B4).

[G] The barrier should be designed at least to absorb kinetic energy E_k = 4724 kJ at the time step when [D] ≥ [E].

Analytical approach	Calculated value	Analytical solution
Impact duration (s)	4.72	$T_s = \frac{\gamma U_0}{\mu g}$
Impact energy (kJ)	2322	$E_B = \frac{\rho Q_0 U_0^3}{4 \mu g}$

Note: γ = 1 is adopted.

[A] Time (s)	Finite Difference Approach					[G] Design Requirement (kJ)
	[B] Vol. of deposit, V _{DAT} (m ³)	[C] Mass of deposit (Kg)	[D] Basal resistance of deposit (KN)	[E] Compaction force from approaching debris, F _A (KN)	[F] Kinetic energy to be absorbed, E _k (KJ)	
0.00	0.00	0	0.00	218.70	0.00	--
0.20	2.70	4860	9.27	218.70	192.66	--
0.40	5.40	9720	18.53	218.70	376.98	--
0.60	8.10	14580	27.80	218.70	552.96	--
0.80	10.80	19440	37.07	218.70	720.59	--
1.00	13.50	24300	46.34	218.70	879.89	--
1.20	16.20	29160	55.60	218.70	1030.85	--
1.40	18.90	34020	64.87	218.70	1173.46	--
1.60	21.60	38880	74.14	218.70	1307.74	--
1.80	24.30	43740	83.41	218.70	1433.67	--
2.00	27.00	48600	92.67	218.70	1551.27	--
2.20	29.70	53460	101.94	218.70	1660.52	--
2.40	32.40	58320	111.21	218.70	1761.43	--
2.60	35.10	63180	120.48	218.70	1854.00	--
2.80	37.80	68040	129.74	218.70	1938.24	--
3.00	40.50	72900	139.01	218.70	2014.13	--
3.20	43.20	77760	148.28	218.70	2081.68	--
3.40	45.90	82620	157.55	218.70	2140.89	--
3.60	48.60	87480	166.81	218.70	2191.75	--
3.80	51.30	92340	176.08	218.70	2234.28	--
4.00	54.00	97200	185.35	218.70	2268.47	--
4.20	56.70	102060	194.62	218.70	2294.32	--
4.40	59.40	106920	203.88	218.70	2311.82	--
4.60	62.10	111780	213.15	218.70	2320.99	--
4.80	64.80	116640	222.42	218.70	2321.81	2321.81
5.00	67.50	121500	231.68	218.70	2314.30	2321.81
5.20	70.20	126360	240.95	218.70	2298.44	2321.81
5.40	72.90	131220	250.22	218.70	2274.24	2321.81
5.60	75.60	136080	259.49	218.70	2241.70	2321.81
5.80	78.30	140940	268.75	218.70	2200.83	2321.81
6.00	81.00	145800	278.02	218.70	2151.61	2321.81
6.20	83.70	150660	287.29	218.70	2094.05	2321.81
6.40	86.40	155520	296.56	218.70	2028.15	2321.81
6.60	89.10	160380	305.82	218.70	1953.90	2321.81
6.80	91.80	165240	315.09	218.70	1871.32	2321.81
7.00	94.50	170100	324.36	218.70	1780.40	2321.81

Table B2 Comparison of the Analytical and Numerical Solutions for Run-up Mechanism

Input parameters for finite difference calculations	
Time increment	0.5 s
Total volume of landside debris	300 m ³
Mass density of landside debris (ρ)	1800 kg/m ³
Discharge rate of landside debris (Q_0)	13.5 m ³ /sec
Velocity of approaching landside debris (U_0)	9 m/sec
Flow depth of approaching landslide debris (h_0)	0.5 m
Inclination of landslide deposit (θ)	11 °
Inclination of debris flow path (α)	0 °
Gravitational acceleration (g)	9.81 m/s ²

Notes:

[A] The time for each calculation step is the time of the previous step plus the time increment.

[B] The height of landslide debris deposited behind the barrier at time, t, is calculated using Equation (B5).

[C] The length of the landslide debris deposited behind the barrier at time, t, is calculated using Equation (14).

[D] Impacting velocity (U_i) of the landslide debris on the flexible barrier is computed using Equation (B6).

[E] The kinetic energy to be absorbed by the barrier ($\Delta E_{k\Delta T}$) in each time step is calculated using Equation (B7).

[F] The total kinetic energy to be absorbed at Time [A] is the sum of [E] in previous calculation time steps until $\Delta E = 0$.

Analytical approach	Calculated value	Analytical solution
Impact energy (kJ)	3196	$E_B = \frac{\rho Q_0 U_0 \cos(\theta - \alpha) \sin(\theta + \alpha)}{h_0 g \mu \cos \theta \sin^2 \theta}$
Impact duration (s)	9.74	$T_s = \frac{U_0^3 \sin(\theta + \alpha) \cos(\theta + \alpha)}{8 h_0 g^2 \sin^2(\theta)}$
Final deposition height (m)	4.13	$H_D = \sqrt{2 U_0 h_0 T_s \tan(\theta + \alpha)}$

Finite Difference Approach					
[A] Time (s)	[B] h_t (m)	[C] X (m)	[D] U_i (m/s)	[E] ΔE (kJ) for Δt	[F] ΣE (kJ)
0	0.00	0.00	9.00	492	492
0.5	0.94	4.81	7.92	381	873
1	1.32	6.80	7.42	334	1207
1.5	1.62	8.33	7.02	299	1506
2	1.87	9.62	6.66	269	1775
2.5	2.09	10.76	6.32	243	2018
3	2.29	11.79	6.00	219	2237
3.5	2.47	12.73	5.70	197	2434
4	2.65	13.61	5.39	177	2611
4.5	2.81	14.43	5.09	158	2769
5	2.96	15.22	4.79	140	2908
5.5	3.10	15.96	4.49	122	3031
6	3.24	16.67	4.18	106	3136
6.5	3.37	17.35	3.85	90	3227
7	3.50	18.00	3.51	75	3302
7.5	3.62	18.63	3.15	60	3362
8	3.74	19.25	2.76	46	3408
8.5	3.86	19.84	2.31	32	3441
9	3.97	20.41	1.77	19	3460
9.5	4.08	20.97	1.01	6	3466
10	4.13	21.24	0.00	0	3466
10.5	4.13	21.24	0.00	0	3466
11	4.13	21.24	0.00	0	3466
11.5	4.13	21.24	0.00	0	3466
12	4.13	21.24	0.00	0	3466
12.5	4.13	21.24	0.00	0	3466
13	4.13	21.24	0.00	0	3466
13.5	4.13	21.24	0.00	0	3466
14	4.13	21.24	0.00	0	3466
14.5	4.13	21.24	0.00	0	3466
15	4.13	21.24	0.00	0	3466
15.5	4.13	21.24	0.00	0	3466

GEO PUBLICATIONS AND ORDERING INFORMATION

土力工程處刊物及訂購資料

A selected list of major GEO publications is given in the next page. An up-to-date full list of GEO publications can be found at the CEDD Website <http://www.cedd.gov.hk> on the Internet under "Publications". Abstracts for the documents can also be found at the same website. Technical Guidance Notes are published on the CEDD Website from time to time to provide updates to GEO publications prior to their next revision.

Copies of GEO publications (except geological maps and other publications which are free of charge) can be purchased either by:

Writing to

Publications Sales Unit,
Information Services Department,
Room 626, 6th Floor,
North Point Government Offices,
333 Java Road, North Point, Hong Kong.

or

- Calling the Publications Sales Section of Information Services Department (ISD) at (852) 2537 1910
- Visiting the online Government Bookstore at <http://www.bookstore.gov.hk>
- Downloading the order form from the ISD website at <http://www.isd.gov.hk> and submitting the order online or by fax to (852) 2523 7195
- Placing order with ISD by e-mail at puborder@isd.gov.hk

1:100 000, 1:20 000 and 1:5 000 geological maps can be purchased from:

Map Publications Centre/HK,
Survey & Mapping Office, Lands Department,
23th Floor, North Point Government Offices,
333 Java Road, North Point, Hong Kong.
Tel: (852) 2231 3187
Fax: (852) 2116 0774

Requests for copies of Geological Survey Sheet Reports and other publications which are free of charge should be directed to:

For Geological Survey Sheet Reports which are free of charge:

Chief Geotechnical Engineer/Planning,
(Attn: Hong Kong Geological Survey Section)
Geotechnical Engineering Office,
Civil Engineering and Development Department,
Civil Engineering and Development Building,
101 Princess Margaret Road,
Homantin, Kowloon, Hong Kong.
Tel: (852) 2762 5380
Fax: (852) 2714 0247
E-mail: jsewell@cedd.gov.hk

For other publications which are free of charge:

Chief Geotechnical Engineer/Standards and Testing,
Geotechnical Engineering Office,
Civil Engineering and Development Department,
Civil Engineering and Development Building,
101 Princess Margaret Road,
Homantin, Kowloon, Hong Kong.
Tel: (852) 2762 5346
Fax: (852) 2714 0275
E-mail: florenceko@cedd.gov.hk

部份土力工程處的主要刊物目錄刊載於下頁。而詳盡及最新的土力工程處刊物目錄，則登載於土木工程拓展署的互聯網網頁 <http://www.cedd.gov.hk> 的“刊物”版面之內。刊物的摘要及更新刊物內容的工程技術指引，亦可在這個網址找到。

讀者可採用以下方法購買土力工程處刊物(地質圖及免費刊物除外):

書面訂購

香港北角渣華道333號
北角政府合署6樓626室
政府新聞處
刊物銷售組

或

- 致電政府新聞處刊物銷售小組訂購 (電話：(852) 2537 1910)
- 進入網上「政府書店」選購，網址為 <http://www.bookstore.gov.hk>
- 透過政府新聞處的網站 (<http://www.isd.gov.hk>) 於網上遞交訂購表格，或將表格傳真至刊物銷售小組 (傳真：(852) 2523 7195)
- 以電郵方式訂購 (電郵地址：puborder@isd.gov.hk)

讀者可於下列地點購買1:100 000、1:20 000及1:5 000地質圖：

香港北角渣華道333號
北角政府合署23樓
地政總署測繪處
電話：(852) 2231 3187
傳真：(852) 2116 0774

如欲索取地質調查報告及其他免費刊物，請致函：

免費地質調查報告：

香港九龍何文田公主道101號
土木工程拓展署大樓
土木工程拓展署
土力工程處
規劃部總土力工程師
(請交：香港地質調查組)
電話：(852) 2762 5380
傳真：(852) 2714 0247
電子郵件：jsewell@cedd.gov.hk

其他免費刊物：

香港九龍何文田公主道101號
土木工程拓展署大樓
土木工程拓展署
土力工程處
標準及測試部總土力工程師
電話：(852) 2762 5346
傳真：(852) 2714 0275
電子郵件：florenceko@cedd.gov.hk

MAJOR GEOTECHNICAL ENGINEERING OFFICE PUBLICATIONS 土力工程處之主要刊物

GEOTECHNICAL MANUALS

Geotechnical Manual for Slopes, 2nd Edition (1984), 300 p. (English Version), (Reprinted, 2011).

斜坡岩土工程手冊(1998)，308頁(1984年英文版的中文譯本)。

Highway Slope Manual (2000), 114 p.

GEOGUIDES

Geoguide 1 Guide to Retaining Wall Design, 2nd Edition (1993), 258 p. (Reprinted, 2007).

Geoguide 2 Guide to Site Investigation (1987), 359 p. (Reprinted, 2000).

Geoguide 3 Guide to Rock and Soil Descriptions (1988), 186 p. (Reprinted, 2000).

Geoguide 4 Guide to Cavern Engineering (1992), 148 p. (Reprinted, 1998).

Geoguide 5 Guide to Slope Maintenance, 3rd Edition (2003), 132 p. (English Version).

岩土指南第五冊 斜坡維修指南，第三版(2003)，120頁(中文版)。

Geoguide 6 Guide to Reinforced Fill Structure and Slope Design (2002), 236 p.

Geoguide 7 Guide to Soil Nail Design and Construction (2008), 97 p.

GEOSPECS

Geospec 1 Model Specification for Prestressed Ground Anchors, 2nd Edition (1989), 164 p. (Reprinted, 1997).

Geospec 3 Model Specification for Soil Testing (2001), 340 p.

GEO PUBLICATIONS

GCO Publication No. 1/90 Review of Design Methods for Excavations (1990), 187 p. (Reprinted, 2002).

GEO Publication No. 1/93 Review of Granular and Geotextile Filters (1993), 141 p.

GEO Publication No. 1/2006 Foundation Design and Construction (2006), 376 p.

GEO Publication No. 1/2007 Engineering Geological Practice in Hong Kong (2007), 278 p.

GEO Publication No. 1/2009 Prescriptive Measures for Man-Made Slopes and Retaining Walls (2009), 76 p.

GEO Publication No. 1/2011 Technical Guidelines on Landscape Treatment for Slopes (2011), 217 p.

GEOLOGICAL PUBLICATIONS

The Quaternary Geology of Hong Kong, by J.A. Fyfe, R. Shaw, S.D.G. Campbell, K.W. Lai & P.A. Kirk (2000), 210 p. plus 6 maps.

The Pre-Quaternary Geology of Hong Kong, by R.J. Sewell, S.D.G. Campbell, C.J.N. Fletcher, K.W. Lai & P.A. Kirk (2000), 181 p. plus 4 maps.

TECHNICAL GUIDANCE NOTES

TGN 1 Technical Guidance Documents